Climate model calculations of the impact of aerosols from road transport and shipping

K.P. Shine[1], E.J. Highwood[1], G. Rädel[1], N. Stuber[1], and Y. Balkanski[2]*

[1]*Department of Meteorology, University of Reading, Earley Gate, Reading RG6 6BB, United Kingdom*
[2]*Lab des Sciences du Climate et de l'Environnement, UMR1572, IPSL, CEA-CNRS-UVSQ, Cedex, France*

Road transport and shipping are copious sources of aerosols, which exert a significant radiative forcing, compared to, for example, the CO_2 emitted by these sectors. An advanced atmospheric general circulation model, coupled to a mixed-layer ocean, is used to calculate the climate response to the direct radiative forcing from such aerosols. The cases considered include imposed distributions of black carbon and sulphate aerosols from road transport, and sulphate aerosols from shipping; these are compared to the climate response due to CO_2 increases. The difficulties in calculating the climate response due to small forcings are discussed, as the actual forcings have to be scaled by large amounts to enable a climate response to be easily detected. Despite the much greater geographical inhomogeneity in the sulphate forcing, the patterns of zonal and annual-mean surface temperature response (although opposite in sign) closely resembles that resulting from homogeneous changes in CO_2. The surface temperature response to black carbon aerosols from road transport is shown to be notably non-linear in scaling applied, probably due to the semi-direct response of clouds to these aerosols. For the aerosol forcings considered here, the most widespread method of calculating radiative forcing significantly overestimates their effect, relative to CO_2, compared to surface temperature changes calculated using the climate model.

Keywords: radiative forcing, climate change, black carbon, transport emissions.

Introduction

The transport sectors (road transport, shipping and aviation) are large and growing sources of a range of emissions of gases and particles that influence climate [1—3]. These emissions include carbon dioxide, oxides of nitrogen (which can influence ozone and methane concentrations), sulphur dioxide (which rapidly forms sulphate aerosols) and black carbon (BC) aerosols. Given international efforts to limit global climate change, there is increasing attention on how emissions from individual sectors might be reduced. It is important that a broad view is taken of the climate impact of each sector, rather than focusing on, for example, CO_2 emissions alone, even if they are often the largest source of radiative forcing. This is to ensure that any mitigation efforts reduce the total climate impact, rather than the climate impact of the CO_2 emissions alone.

The climate impact of CO_2 from the transport sectors is no different to the impact of CO_2 from any other anthropogenic source, because it is a long lived gas and hence quite well mixed in the atmosphere. By contrast, aerosol and aerosol precursors are much shorter lived (atmospheric lifetimes typically around one week) and, because of the inhomogeneous distribution of these sources, their distribution in the atmosphere is also inhomogeneous. Hence it is in principle necessary to compute the climate response to aerosols from each source separately to understand the extent to which this inhomogeneity impacts on the climate response.

The work reported here was performed as part of the European Union Integrated Project QUANTIFY (Quantifying the Climate Impact of Global and European Transport Systems). The year 2000 radiative forcing due to aerosols resulting from the transport sectors has been reported in detail [4]. That study considered the forcing due to BC, sulphate and organic carbon aerosols for the three sectors; it considered only the direct impact of the aerosols on the radiation budget, rather than the indirect aerosol effects on cloud properties, which is particularly uncertain [1]. The framework adopted here does not include these indirect cloud effects but it does allow for the so-called semi-direct response of clouds to aerosols, which is particularly important for BC and is strongly dependent on the altitude of the BC [5, 6]; changes in the heating rate due to the presence of the absorbing aerosol impact on temperatures, relative humidity and atmospheric stability, which can then influence the amounts and properties of clouds, with subsequent effects on its radiative forcing. (The simulations reported here do not, however, include any effect of surface deposition of BC on the surface albedo, which also may have a significant influence on climate response [6].)

The dominant contributors to the direct global-mean aerosol radiative forcing calculated by [4] were BC from the road sector (around 25—60 mW·m^{-2} depending on the method used) and sulphate from the shipping sector (−23 to −30 mW·m^{-2}) with sulphate

---

* K.P. Shine (k.p.shine@reading.ac.uk).

from road contributing -7 to -12 mW $\cdot$ m^{-2}. All the other aerosol direct radiative forcings due to the transport sector were calculated to be much smaller (magnitudes of 4 mW $\cdot$ m^{-2} or less) and so are not considered further here. For reference, the year 2000 CO_2 forcing has been estimated to be 150, 34, 25 mW $\cdot$ m^{-2} for the road transport, shipping and aviation sectors respectively [1—3]. These show that the aerosol forcings for the road and shipping sectors are significant fractions of the CO_2 forcing.

Part of the motivation for this paper is to explore some of the difficulties in using climate models to assess the impact of radiative forcing from individual sectors. One particular problem is that the radiative forcings from the transport sectors are relatively small; and when imposed on a climate model, the response would be small compared to the model's interannual variability. In principle, the model could be integrated for very long periods, to help detect a signal, but this is computationally expensive. Instead, it is common [7—9] to scale the perturbation in concentrations resulting from a given sector by some scaling factor, typically of order 10^2 to 10^3, so that the forcing is around several W $\cdot$ m^{-2}. This allows a detectable climate response to be obtained using a shorter integration time. This is the method adopted here. It raises questions about the linearity of both the forcing and the climate response — these issues will be discussed.

Climate model

The experiments use the UK Met Office HadSM3 climate model [10], which comprises the atmosphere general circulation model HadAM3 coupled to a slab ocean of 50 m depth. HadSM3 is, relatively, a computationally inexpensive tool to study the equilibrium response to climate perturbations and has been shown to give a reasonable representation of the response of a more fully-coupled atmosphere-ocean general circulation model [10]. The atmospheric model has a horizontal resolution of $3.75° \times 2.5°$ and 19 vertical levels. As ocean dynamics are not included in HadSM3, surface heat fluxes have to be adjusted to obtain a realistic representation of sea ice and sea surface temperatures. These heat fluxes are taken to represent the convergence of heat due to ocean heat transport; once the values are derived in a calibration run of the model, they are then assumed to be fixed in both the control and perturbation runs of the model. Details of the method can be found in [11, 12]. HadAM3 uses the prognostic cloud scheme described by [13, 14]. Cloud amount, cloud ice, and cloud water are diagnosed from total moisture content and liquid-water potential temperature. HadAM3, and the radiative forcing calculations reported here, use the same radiation scheme [15]. A control simulation of 55 years in length is performed, with no imposed radiative forcing; this provides the reference with which to compare the effects of the aerosol perturbations. The climate model integrations with perturbed aerosol dis-

tributions were 35 years in length. The regression analysis discussed in the next section used the first 20 years of the perturbed run and the equilibrium climate response was calculated using the last 15 years.

The monthly-mean sulphate and BC aerosol distributions used here are taken from the simulations labelled LSCE in [4]. Note that these are fixed aerosol distributions which do not interact with the climate model meteorology; hence in the simulations reported here, the aerosols impact on the climate but there is no feedback from the computed climate change on the aerosol distribution. An additional calculation is presented here for a doubling of CO_2 (from its control value of 277 ppmv); this acts as a convenient reference point because it is a standard experiment in climate models.

Analysis framework

The basic framework for the global-mean analysis assumes that the equilibrium surface temperature ΔT (in K) is linearly proportional to the radiative forcing, RF (in W $\cdot$ m^{-2}) so that

$$\Delta T = \lambda RF, \qquad (1)$$

where λ is the climate sensitivity $\left(\text{in } K \; (W \cdot m^{-2})^{-1}\right)$. While this basic framework has been in place for many decades, there have been significant recent modifications to it, partly driven by the need to understand the more complicated response of models to changes in BC, compared to "simpler" forcings such as changes in CO_2, and to facilitate easier diagnosis of climate model experiments [6, 16—19]. The standard definition of radiative forcing used, for example, in Intergovernmental Panel on Climate Change assessments [20] is calculated assuming that all surface and tropospheric parameters are held fixed (with the exception of the parameter causing the forcing) but with stratospheric temperatures allowed to adjust to the forcing — this gives the so-called adjusted radiative forcing, that will be labelled RF_{adj}. The rationale for the inclusion of this adjustment is that the stratosphere responds relatively quickly (in a few months) to the imposition of a perturbation, while the tropospheric response is of order decades, and is dictated by the timescale for the oceans to respond. For the aerosol direct forcings considered here, the effect of stratospheric temperature adjustment is of minor importance.

More recently, it has come to be appreciated that, as well as the slow response of the troposphere to changes in ocean temperature, there are a number of tropospheric "fast feedbacks" not resulting from the surface warming that are, conceptually, better considered as part of the forcing. This is particularly so for BC forcing where it has been found that Equation (1) can sometimes fail to predict even the sign of ΔT if RF_{adj} is used [5, 6], because, primarily, of the rapid semi-direct response of clouds. A range of alternative definitions of radiative forcing have been proposed [6, 16, 17]. One that is relatively easy to apply to climate model output is described in [17] and is used here. This method determines a radiative

forcing (RF_{reg}) and climate sensitivity parameter (λ_{reg}) by regressing the global- and annual-mean top-of-atmosphere radiative flux against ΔT as the model evolves towards a new equilibrium after a radiative forcing has been applied. The intercept of the regression line with the y-axis gives RF_{reg} while the λ_{reg} is given by the slope of the line. Because a regression is performed on noisy model data, there is a statistical uncertainty in the derived parameters, which depends on the size of the initial forcing. λ_{reg} is used here in addition to the "standard" climate sensitivity, λ_{adj}, derived using the RF_{adj} and Equation (1).

The regression method has been extended [18] to derive radiative forcings and climate sensitivities for clear and cloudy skies and for longwave and short-wave fluxes separately, which provides important additional information on the model response.

An additional modification to the framework represented by Equation (1) is that in early work on climate response it was assumed that λ was independent of the radiative forcing mechanism. With the study of a wider range of forcing mechanisms in recent years it is now appreciated that this is not the case [6, 19] and indeed that λ also depends on the size of the forcing [6, 9]; in one model [9] the change is clearly related to a weakening of the negative cloud feedback as the forcing increases. This dependence has been characterised by the efficacy, E_{reg}, which is defined here as being the climate sensitivity for a given radiative forcing relative to the climate sensitivity for a doubling of CO_2: $E_{reg} = \lambda_{reg}/\lambda_{reg}(2 \times CO_2)$. An efficacy, E_{adj}, using the values of λ_{adj}, can also be derived.

Global-mean results

Table 1 shows the global-mean values for RF_{reg}, RF_{adj}, ΔT, λ_{reg}, λ_{adj}, E_{reg}, and E_{adj}. Climate model results are presented for $2 \times CO_2$, BC from road transport using scaling factors of 250, 500 and 1000, and road and ship sulphate with scaling factors of 1000. The values of RF_{adj} with no scalings (as given in [4]) are also shown.

Considering first the BC calculations, there are several features of note. As expected for an absorbing aerosol, the forcing is positive. RF_{reg} is typically 40% of RF_{adj}; this ratio is surprisingly constant amongst the simulations, given the potential non-linearities in the fast feedbacks involving clouds. The causes of the difference between RF_{reg} and RF_{adj} and, in particular, the longwave and shortwave and clear and cloudy components, can be used to understand the model behaviour (Table 2).

Considering the $500 \times$ BC case, the shortwave RF_{reg} is 7.5 $W \cdot m^{-2}$, which is 75% of RF_{adj} but this is significantly offset by a -3.2 $W \cdot m^{-2}$ cloudy-sky longwave forcing. Since the BC RF_{adj} does not have a longwave component (the BC particles being too small to exert a significant influence), the longwave component of RF_{adj} has to be interpreted as a "fast feedback" in cloud amount [18] in response to the BC, as a result of the semi-direct dissipation of cloud; a similar large longwave response has been found in earlier climate model experiments [20]. The fact that even the shortwave RF_{reg} is smaller than RF_{adj} is also consistent with this. Cloud can either enhance the direct shortwave BC forcing, if there is sufficient BC above a cloud, or decrease it, if it is mostly below cloud [21] — in these simulations there is sufficient above-cloud BC for the cloudy-sky RF_{adj} to exceed the clear-sky RF_{adj} (for the $1 \times$ BC case the clear sky RF_{adj} is 20 $mW \cdot m^{-2}$, compared to the total RF_{adj} of 24 $mW \cdot m^{-2}$ (Table 1)); hence a decrease in cloud amount also leads to a decreased shortwave forcing in this case. Similar behaviour is found in the BC runs using the other scaling (Table 2).

Table 1 shows that neither version of RF is linear in the scaling factor; for example, RF_{adj} for a scaling factor of 1000 is around 25% lower than $1000 \times RF_{adj}$ for a scaling factor of 1. This is because of the very inhomogeneous distribution of BC [4]; linearity would only be expected if the optical depth was low (much less than 1), which is not the case in heavily polluted regions. Figure 1 shows RF_{adj} as a function of scaling factor for both the global mean, and two regions — the more heavily polluted

Table 1

Global-mean impact of CO_2 changes and the black carbon (BC) and (direct) sulphate forcing from road and shipping, for various applied scaling factors. Radiative forcing, climate sensitivity and efficacy are shown for both the standard definition of radiative forcing (subscript *adj*) and the regression technique (subscript *reg*). The global-mean surface temperature change is also shown. Climate model calculations are not performed for the "1×" experiments so only the adjusted forcing is shown. The uncertainty in RF_{reg} is given (in parentheses) by the standard error of the regression. The uncertainty in λ_{reg} (in parentheses) comes from the root-mean square deviation in the slope of the regression line

Experiment	RF_{reg}, $W \cdot m^{-2}$	RF_{adj}, $W \cdot m^{-2}$	ΔT, K	λ_{reg}, $K \cdot (W \cdot m^{-2})^{-1}$	λ_{adj}, $K \cdot (W \cdot m^{-2})^{-1}$	Efficacy E_{reg}	Efficacy E_{adj}
$2 \times CO_2$	4.0 (0.1)	3.8	3.4	0.84 (0.01)	0.89	1	1
$1 \times$ road BC	—	0.024	—	—	—	—	—
$250 \times$ road BC	2.6 (0.3)	5.6	0.9	0.45 (0.06)	0.16	0.54	0.18
$500 \times$ road BC	3.9 (0.4)	10.1	2.1	0.63 (0.04)	0.20	0.75	0.22
$1000 \times$ road BC	7.7 (0.2)	17.4	5.7	0.81 (0.00)	0.33	0.96	0.37
$1 \times$ road SO_4	—	−0.009	—	—	—	—	—
$1000 \times$ road SO_4	−6.7 (0.1)	−8.5	−3.0	0.58 (0.00)	0.35	0.69	0.39
$1 \times$ ship SO_4	—	−0.026	—	—	—	—	—
$1000 \times$ ship SO_4	−18.9 (0.1)	−20.0	−9.2	0.66 (0.00)	0.46	0.79	0.52

Shine K.P., Highwood E.J., Rädel G., et al.

Longwave and shortwave, and clear and cloudy, components of the RF_{reg} (in $W \cdot m^{-2}$) (top part of table) and the climate feedback parameter (in $W \cdot m^{-2} \cdot K^{-1}$) (bottom part of table) for the $2 \times CO_2$ case and the three road BC cases. The climate feedback parameter is presented as the negative of the reciprocal of the climate sensitivity parameter shown in Table 1; it is presented in this way because the individual components of the reciprocal can be added to obtain the net, following the sign convention in [18]. The figures in parentheses are the statistical uncertainties in the regressions, as described in the caption to Table 1

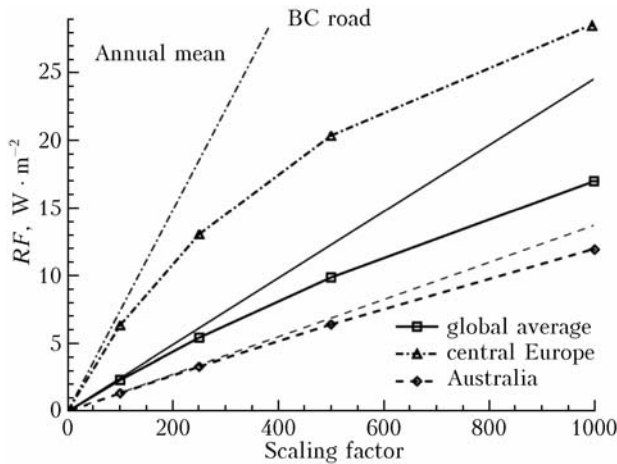| Forcing	LW_{clear}	SW_{clear}	LW_{cloudy}	SW_{cloudy}	Total
$2 \times CO_2$	−4.0 (0.01)	−0.2 (0.005)	−0.9 (0.005)	1.1 (0.06)	4.0
$250 \times$ road BC	−0.42 (0.02)	2.5 (0.02)	−1.6 (0.02)	2.1 (0.4)	2.6
$500 \times$ road BC	−0.45 (0.03)	4.7 (0.01)	−3.2 (0.02)	2.8 (0.04)	3.9
$1000 \times$ road BC	−0.50 (0.15)	7.9 (0.003)	−6.1 (0.03)	5.3 (0.22)	7.6
Feedback					
$2 \times CO_2$	−2.0 (0.001)	0.7 (0.001)	0.2 (0.001)	−0.04 (0.007)	−1.2
$250 \times$ road BC	−2.0 (0.02)	1.0 (0.02)	0.0 (0.01)	−1.2 (0.3)	−2.2
$500 \times$ road BC	−1.8 (0.01)	0.7 (0.002)	0.1 (0.003)	−0.6 (0.08)	−1.6
$1000 \times$ road BC	−1.8 (0.01)	0.5 (0.001)	0.3 (0.001)	−0.3 (0.01)	−1.2

Fig. 1. RF_{adj} (lines with symbols) versus scaling factor for road BC aerosols for the global average, a heavily polluted region (central Europe) and a less polluted region (Australia). The lines without symbols show the same cases assuming the forcing is linear in scaling factor, using RF_{adj} with a scaling factor of 1

central Europe and the less polluted Australian region. For central Europe there is a very marked deviation from linearity, while for Australia it is only of order 10% — this also has implications for the geographical distribution of the forcing as the scaling is changed (see next section).

Table 1 also shows that E_{reg} for the BC forcing varies markedly with scaling factor; for a scaling factor of 250, the BC forcing is only half as effective as $2 \times CO_2$, while for a factor of 1000, E_{reg} is close to 1. This is consistent with earlier climate model experiments [6, 9] indicating that λ increases with the size of the forcing. Using the decomposition of climate sensitivity into clear and cloudy, and shortwave and longwave, using the regression technique [18], the cause of this behaviour can be analysed (Table 2) where

the (negative) reciprocal of the climate sensitivity is presented as this means the different components can be added to obtain the total reciprocal of the climate sensitivity [18]. The most notable change is in the cloudy shortwave climate feedback parameter — this component is negligible in $2 \times CO_2$ calculations [8] but is a strong negative feedback for the $250 \times$ case which weakens as the BC scaling factor increases. Although the diagnostics are not available to fully establish the cause, one plausible explanation concerns the shift of mixed-phase clouds in the model towards being more liquid than ice, a mechanism which has been shown to be a potentially powerful negative feedback mechanism [22]. The extra shortwave absorption due to the presence of the BC leads to an increase in atmospheric temperature which may enhance the effectiveness of this feedback as surface temperatures increase; however, as the temperature increases further, and the conversion to liquid is more or less complete in the mixed-phase clouds, this feedback would be expected to weaken, as is found for the higher BC scaling factors.

The change in efficacy with forcing is much stronger in this BC case than for any of the cases (including ozone and CO_2 changes) shown by [6, 9] The simulations raise serious questions about how the climate response to road BC can be compared with the climate response of CO_2 from the same sector. Considering RF_{adj} alone, which has been a conventional method of comparing different climate forcing mechanisms, road BC enhances the road CO_2 forcing by around 16% (although, as noted in the Introduction, the results in [4] indicate it could be 40%). The climate model results indicate that E_{adj} is much less than unity, due to a combination of the fact that RF_{reg} is much smaller than RF_{adj} and the fact that E_{reg} is much less than one. [9] report an example (for ozone forcing from the transport sectors) where the efficacy is (quadratically) extrapolated back to small values

of forcing, to infer a value that is appropriate for the actual values of the forcing. Unfortunately in the BC case presented here, the curvature of a plot of efficacy versus forcing is such that any extrapolation is unlikely to be reliable. Nevertheless, the climate model simulations presented here indicate that the effect of road BC on surface temperatures might be only one quarter of that indicated by RF_{adj}. Because different climate models are likely to have different responses to the imposition of BC, it is unsafe to draw firm conclusions from the results from one climate model, but nevertheless the results here indicate the need for further experimentation.

Previous climate model results on the efficacy of fossil-fuel (rather than specifically road transport) BC emissions generally indicate an efficacy less than 1 (at least in the absence of the effect of deposition of BC on surface albedo). Interpretation is not straightforward as different distributions of BC have been used and the definition (and size) of the forcing differs. Using the adjusted forcing, [23] and [6] found $E_{adj} = 0.61$ and 0.78 respectively; using approaches that approximate to E_{reg}, [24] and [6] obtained 0.71 (but with large uncertainty as their applied forcing was small ($0.4 \text{ W} \cdot \text{m}^{-2}$)) and 0.93 respectively. The range of values for E_{reg} is not dissimilar to those found here, but the E_{adj} values found here are certainly lower.

Table 1 also shows the negative forcing and surface cooling for the sulphate experiments. As expected the difference between RF_{reg} and RF_{adj} is much smaller, because the fast feedbacks are less effective than for BC. The non-linearity is less marked, especially in the road case, as a result of the lower aerosol abundances. The efficacies in the sulphate experiments are markedly lower than unity in both cases and lower than would be found for the equivalent size of forcing in the BC case. Part of the explanation for the low efficacy could be that, in some climate models at least, radiative forcings concentrated in the tropics have a lower efficacy than globally distributed forcings [25] and the road and ship sulphate forcings are more strongly peaked in the sub-tropics than the CO_2 forcing (see Figure 2).

Although less extreme than the BC case, these experiments also indicate that using RF_{adj} to compare the direct sulphate forcing and CO_2 forcing from the transport sector may overestimate the influence of sulphate on surface temperature by a factor of 2.
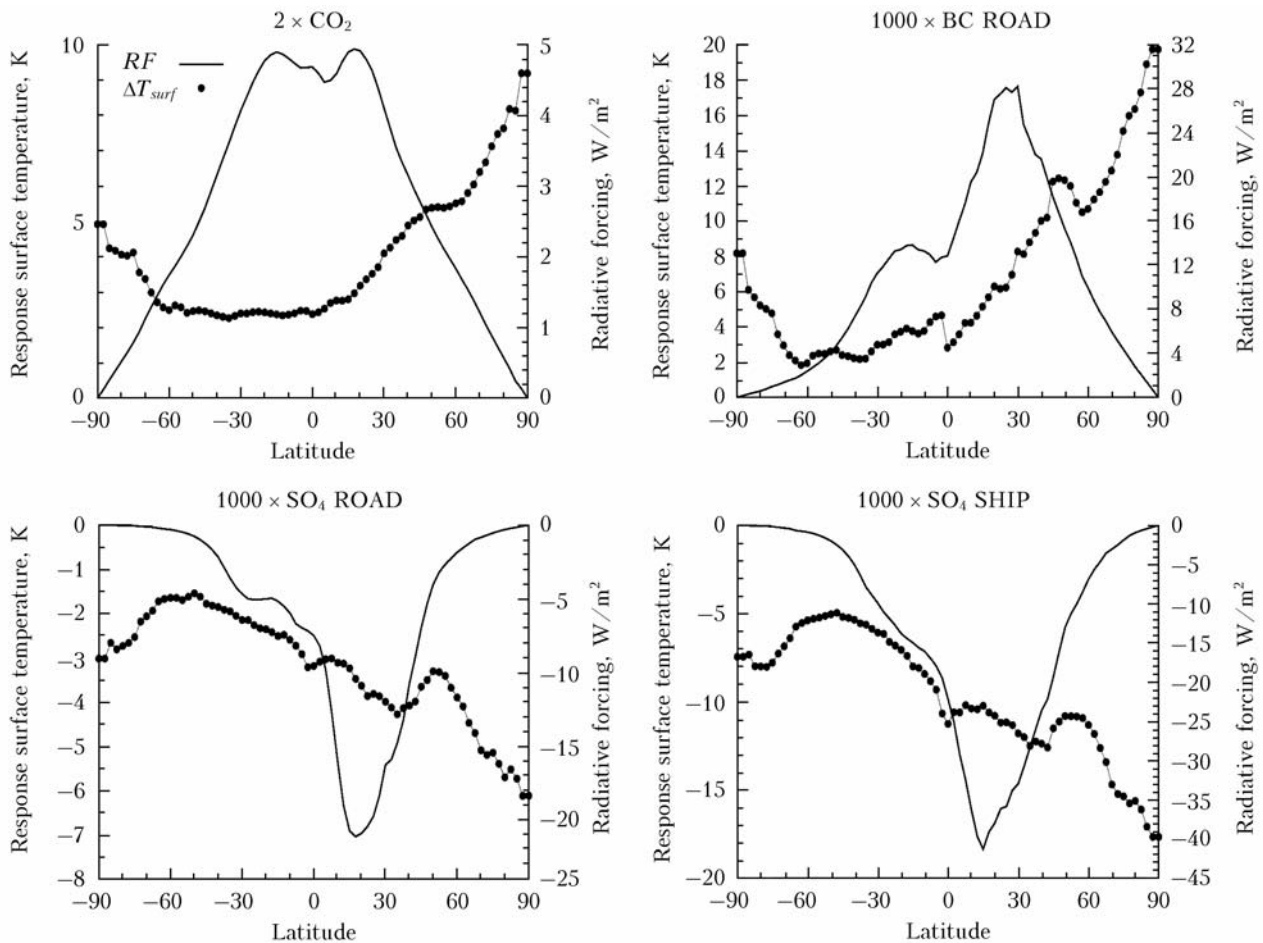

Fig. 2. Annual and zonal-mean RF_{adj} and ΔT as a function of latitude for $2 \times CO_2$ (top left), $1000 \times$ road BC (top right), $1000 \times$ road sulphate (bottom left) and $1000 \times$ ship sulphate (bottom right). For ΔT, a symbol is only plotted when the change from the control integration is statistically significant at 95%, using a t-test

Shine K.P., Highwood E.J., Rädel G., et al.

Zonal-mean surface temperature response

Figure 2 shows the annual and zonal-mean surface temperature response, together with RF_{adj}, for the $2 \times CO_2$ case and the three 1000× scaling factor cases (road BC, road sulphate and shipping sulphate). Because the aerosol emission sources are largely concentrated in the northern hemisphere, so too are the forcings, with peaks in the northern hemisphere sub-tropics.

As expected from earlier climate model studies [6, 25, 26] the surface temperature response is quite distinct from the pattern of forcing and is dictated more by the pattern of climate feedbacks. The peak response is at northern high latitudes in all three cases, with a significant southern hemisphere response, and indeed the patterns of response are similar in all three cases, although the sign of the response depends on the sign of the forcing. These results re-emphasize an important point that it is not correct to assume the pattern of climate response follows simplistically from the pattern of the imposed forcing; even quite geographically constrained forcings can have a global reach in terms of their impact. Indeed, the ratio of northern to southern hemispheric mean temperature change is almost identical in the $2 \times CO_2$ experiment (where it is 1.7) compared to the two sulphate experiments (where it is 1.8) despite the marked difference in the pattern of the forcing.

A noteable aspect of the three BC experiments is the change in geographical pattern of the response as the scaling factor increases. Figure 3 shows the response for scalings of 250× and 1000×, together with the 250× case multiplied by the ratio of the global-mean RF_{reg} forcings shown in Table 1 for factors of 1000× and 250× (i.e. 3.1).
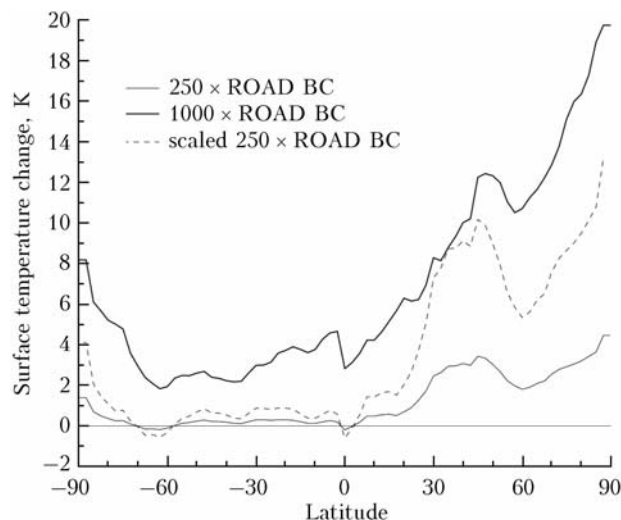

Fig. 3. Annual and zonal mean ΔT for road BC for scaling factors of 250 and 1000. Also shown is the scaling factor 250 case multiplied by the ratio of the annual and global mean RF_{reg} for the two cases (taken from Table 1)

If the response was linear in radiative forcing, the results for the 250× case, multiplied by 3.1, would be approximately the same as the 1000× case. It is clear from Table 1 that this is not even the case for global mean ΔT (the ratio is almost double, at 6.3), related to the increase in λ with forcing noted earlier. Figure 3, though, shows that in addition to this global-mean effect, there are large latitudinal variations in the response. Of particular note is that the 1000× case has a far greater relative response than the 250× case in the southern hemisphere.

The cause of the amplified southern hemisphere response seems likely to be due to non-linearities in the semi-direct response of clouds, as BC concentrations are increased. A possible contributor to this response is the difference in the height distribution of BC in the two hemispheres. In the northern hemisphere, where most of the BC is emitted, the aerosol is predominantly in the boundary layer at pressures greater than 800 hPa. By contrast, most of the southern hemisphere BC is in the tropical upper troposphere, advected there in the upper branch of the Hadley circulation during northern hemisphere summer. This difference in height distribution may trigger different fast feedbacks in the two hemispheres; it is likely to be mostly low cloud affected in the northern hemisphere and mostly high cloud in the southern hemisphere. It is of interest that the asymmetry found in the surface temperature response is not found in the upper troposphere (Figure 4), again indicating that the two hemispheres are responding in different ways, because of the nature of BC forcing differs between them.
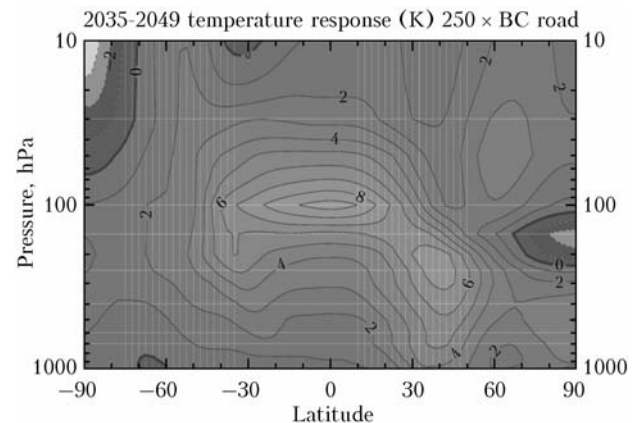

Fig. 4. Annual and zonal-mean temperature response as a function of latitude and pressure for the $250 \times BC$ case. The contour interval is 1 K

It is notable that other climate model calculations of the impact of BC (from all anthropogenic sources) [24] also found a muted surface temperature response in the southern hemisphere mid-latitudes, relative to other forcings, when a small BC forcing is applied, as is found for the 250× case here.

One additional potential contributor comes from the non-linearity of the forcing to the scaling factor, discussed above. The northern hemisphere forcing increases less rapidly with scaling factor (because of the larger optical depth) than the southern hemisphere forcing — this is illustrated in Figure 5, where the

2. Оптика атмосферы и океана, № 6.

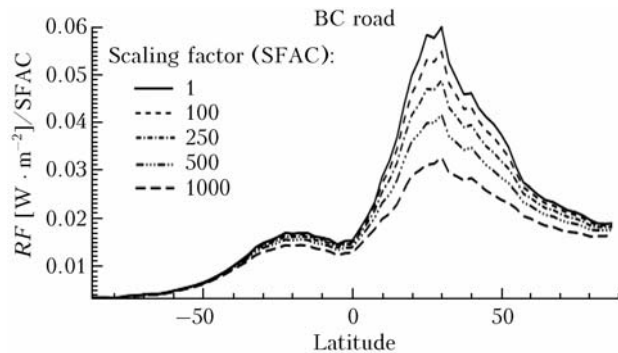annual and zonal-mean RF_{adj} divided by the scaling factor is plotted.

Fig. 5. Annual and zonal-mean RF_{adj} divided by the scaling factor (SFAC) for 5 scaling factors using the BC road distributions

It is clear that the southern hemisphere forcing becomes relatively more important as the scaling factor increases — the ratio of the northern to southern hemispheric mean RF_{adj} is 3.3, 2.8, 2.6, and 2.3 for scaling factors of 1, 250×, 500×, and 1000×. However, the corresponding ratios for the hemispheric-mean ΔT are 9.4, 4.7, and 2.1 for scaling factors of 250×, 500×, and 1000× respectively, indicating a much more rapid change with scaling factor than is found for the forcings.

Conclusions

It is important to emphasize that results presented here are from a single climate model and similar calculations using other climate models may lead to significantly different conclusions. Nevertheless, the results raise important issues on how the climate impact of radiative forcings from individual sectors can be compared.

The first issue is that the use of the standard method of calculation of radiative forcing, RF_{adj}, to compare the aerosol forcings with CO_2 forcings, appears to overestimate their impact on global-mean surface temperature by between 2 and 4. This results from a combination of the fact that the radiative forcing apparently felt by the model, RF_{reg} is less than RF_{adj} and the climate sensitivity of RF_{reg} is lower for the aerosol forcings than for CO_2. This may be related to the fact that these aerosol forcings are more strongly peaked in the sub-tropics, compared to CO_2 forcing; earlier studies have shown that this tends to be associated with a smaller efficacy.

The second issue that has been explored here in the context of black carbon forcing is the response to the chosen scaling factor, which was applied in order to achieve a detectable climate response, is highly non-linear. Not only does the efficacy of the black carbon increase as the scaling factor increases, but there is a substantial change in the geographical response, with the southern hemisphere surface temperature change increasing more rapidly with scaling factor than does the forcing itself. These results make it difficult to reliably extrapolate the temperature responses back to the actual (rather than the scaled) forcings.

The third issue is the re-affirmation of a conclusion from previous climate model studies, that the pattern of surface temperature response bears little resemblance to the radiative forcing pattern. Indeed, the pattern of climate response to sulphate forcing closely resembles (although it is, of course, of opposite sign) the pattern resulting from a change in CO_2 despite the very marked differences in the geographical pattern of the forcing itself.

The results here indicate the need for further experimentation with other climate models, especially to ascertain whether the efficacies deduced here are representative of a wider range of climate models. If they were, it would have significant implications for the way non-CO_2 forcings from the transport sector are compared with the CO_2 forcings, which could influence proposed mitigation strategies.

References

1. Eyring V., Isaksen I.S.A., Berntsen T., Collins W.J., Corbett J.J., Endresen O., Grainger R.G., Moldanova J., Schlager H., and Stevenson D.S., "Transport impacts on atmosphere and climate: shipping," *Atmos. Environ.*, **44**, 4735–4771 (2010).
2. Lee D.S., Pitari G., Grewe V., Gierens K., Penner J.E., Petzold A., Prather M.J., Schumann U., Bais A., Berntsen T., Iachetti D., Lim L.L., and Sausen R., "Transport impacts on atmosphere and climate: aviation," *Atmos. Environ.*, **44**, 4678–4734 (2010).
3. Uherek E., Halenka T., Borken-Kleefeld J., Balkanski Y., Berntsen T., Borrego C., Gauss M., Hoor P., Juda-Rezler K., Lelieveld J., Melas D., Rypdal K., Schmid S., "Transport impacts on atmosphere and climate: land transport," *Atmos. Environ.*, **44**, 4772–4816 (2010).
4. Balkanski Y., Myhre G., Gauss M., Rädel G., Highwood E.J., and Shine K.P., "Direct radiative effect of aerosols emitted by transport: from road, shipping and aviation," *Atmos. Chem. Phys.*, **10**, 4477–4489 (2010).
5. Cook J. and Highwood E.J., "Climate response to tropospheric aerosols in an Intermediate General Circulation Model," *Q. J. R. Meteorol. Soc.*, **130**, 175–191 (2004).
6. Hansen J., Sato M., Ruedy R., Nazarenko L., Lacis A., Schmidt G.A., Russell G., Aleinov I., Bauer M., Bauer S., Bell N., Cairns B., Canuto V., Chandler M., Cheng Y., Del Genio A., Faluvegi G., Fleming E., Friend A., Hall T., Jackman C., Kelley M., Kiang N.Y., Koch D., Lean J., Lerner J., Lo K., Menon S., Miller R.L., Minnis P., Novakov T., Oinas V., Perlwitz Ja., Perlwitz Ju., Rind D., Romanou A., Shindell D., Stone P., Sun S., Tausnev N., Thresher D., Wielicki B., Wong T., Yao M., and Zhan S., "Efficacy of climate forcings," *J. Geophys. Res.*, **110**, D18104 (2005).
7. Rind D., Lonergan P., and Shah K., "Climatic effect of water vapor release in the upper troposphere," *J. Geophys. Res.*, **101**, 29395–29405, doi: 10.1029/96JD02747 (1996).

8. Ponater M., Marquart S., Sausen R., and Schumann U., "On contrail climate sensitivity," *Geophy. Res. Lett.*, **32**, L10706 (2005).

9. Ponater M., Dietmüller S., Stuber N., Shine K.P., Highwood E.J., and Rädel G., "Indications of distinctive efficacies for transport related ozone perturbations," Pp. 95–101 in *Proc. of the 2nd International Conference on Transport, Atmosphere and Climate* (Eds. R. Sausen, P.F.J. van Velthoven, C. Brüning, A. Blum) Forschungbericht 2010–10, Deutches Zentrum für Luft und Raumfurht, Munich (http://www.pa.op.dlr.de/tac/2009/proceedings.html) (2010).

10. Williams K.D., Senior C.A., and Mitchell J.F.B., "Transient climate change in the Hadley Centre models: The role of physical processes," *J. Climate*, **14**, 2659–2674 (2001).

11. Gordon C., Cooper C., Senior C.A., Banks H., Gregory J.M., Johns T.C., Mitchell J.F.B., and Wood R.A., "The simulation of SST, sea ice extents and ocean heat transports in a version of the Hadley Centre coupled model without flux adjustments," *Clim. Dyn.*, **16**, 147–168 (2000).

12. Pope V.D., Gallani M.L., Rowntree P.R., and Stratton R.A., "The impact of new physical parametrizations in the Hadley Centre climate model: HadAM3," *Clim. Dyn.*, **16**, 123–146 (2000).

13. Smith R.N.B., "A scheme for predicting layer clouds and their water content in a general circulation model," *Q. J. R. Meteorol. Soc.*, **116**, 435–460 (1990).

14. Gregory D. and Morris D., "The sensitivity of climate simulations to the specification of mixed phase clouds," *Clim. Dyn.*, **12**, 641–651 (1996).

15. Edwards J.M. and Slingo A., "Studies with a flexible new radiation code. I: Choosing a configuration for a large-scale model," *Q. J. R. Meteorol. Soc.*, **122**, 689–719 (1996).

16. Shine K.P., Cook J., Highwood E.J., and Joshi M.M., "Alternative to radiative forcing for estimating the relative importance of climate change mechanisms," *Geophys. Res. Lett.*, **30**, 2047 (2003).

17. Gregory J.M., Ingram W.J., Palmer M.A., Jones G.S., Stott P.A., Thorpe R.B., Lowe J.A., Johns T.C., and Williams K.D., "A new method for diagnosing radiative forcing and climate sensitivity," *Geophys. Res. Lett.*, **31**, L03205 (2004).

18. Gregory J. and Webb M., "Tropospheric adjustment induces a cloud component in CO_2 forcing," *J. Climate*, **2**, 58–71 (2008).

19. Forster P., Ramaswamy V., Artaxo P., Berntsen T., Betts R., Fahey D.W., Haywood J., Lean J., Lowe D.C., Myhre G., Nganga J., Prinn R., Raga G., Schulz M., and Van Dorland R., Changes in atmospheric constituents and in radiative forcing, in *Climate Change 2007: The Physical Science Basis. Contribution of Working Group I to the Fourth Assessment Report of the Intergovernmental Panel on Climate Change*, Edited by S. Solomon, D. Qin, M. Manning, Z. Chen, M. Marquis, K.B. Averyt, M. Tignor, and H.L. Miller, pp. 129–234, Cambridge Univ. Press, Cambridge, UK and New York, USA (2007).

20. Penner J.E., Zhang S.Y., and Chuang C.C., "Soot and smoke aerosol may not warm climate," *J. Geophys. Res.*, **108**, 4657 (2003).

21. Haywood J. M. and Ramaswamy V., "Global sensitivity studies of the direct radiative forcing due to anthropogenic sulphate and black carbon aerosols," *J. Geophys. Res.*, **103**(D6), 6043–6058 (1998).

22. Mitchell J.F.B., Senior C.A., and Ingram W.J., "CO_2 and climate: A missing feedback?," *Nature*, **341**, 132–143 (1989).

23. Roberts D.L. and Jones A., "Climate sensitivity to black carbon aerosol from fossil fuel combustion," *J. Geophys. Res.*, **109**, D16202 (2004).

24. Jones A., Haywood J.M., and Boucher O., "Aerosol forcing, climate response and climate sensitivity in the Hadley Centre climate model," *J. Geophys. Res.*, **112**, D20211 (2007).

25. Joshi M., Shine K., Ponater M., Stuber N., Sausen R., and Li L., "A comparison of climate response to different radiative forcings in three general circulation models: towards an improved metric of climate change," *Clim. Dyn.*, **20**, 843–854 (2003).

26. Boer G.J. and Yu B., "Climate sensitivity and response," *Clim. Dyn.*, **20**, 415–429 (2003).